

# SERIES RESONANT CONVERTER WITH WIDE LOAD RANGE

Leopoldo Rossetto\* and Giorgio Spiazzi\*\*

\* *Department of Electrical Engineering, University of Padova*

\*\* *Department of Electronics and Informatics, University of Padova*

*Via Gradenigo 6A - 35131 Padova - ITALY*

*Tel. (+39-49) 827-7517 - Fax (+39-49) 827-7599/7699*

*email: pel@dei.unipd.it*

**Abstract.** A modification of the series resonant converter topology is presented which extends converter operation from no-load to full-load. This result is accomplished by adding two switches at the secondary-side bridge rectifier, thus improving output voltage control. The resonant inverter can be operated either at constant switching frequency, even for the half-bridge topology, or at variable switching frequency. With constant switching frequency, the output voltage is regulated by controlling the switches of the rectifier stage.

Soft-switching commutations of all switches are maintained in any operating condition, thus optimizing overall efficiency.

The secondary-side control of the output voltage adds another interesting feature to the basic converter, i.e. the step-up and step-down regulation capability which allows the use of this topology in high power factor rectification, too.

Simulated and experimental results confirm proper converter operation in the range from no-load to full-load.

## I. INTRODUCTION

Series resonant converters, operated above the resonant frequency, show many advantages: inherent short circuit protection, zero-voltage commutations, limited harmonics in the resonant current, maximum power transfer at minimum switching frequency, transformer leakage inductance included in the resonant link, etc. Their main limitation is that, for reduced load current, they lose the soft commutation advantage and the output voltage cannot be controlled anymore. Moreover, converter transfer function strongly depends on the load value.

The paper presents a modification of the basic converter topology which allows the extension of the converter operation down to no-load condition, while maintaining all the good characteristics of the basic topology. Moreover some additional features are obtained:

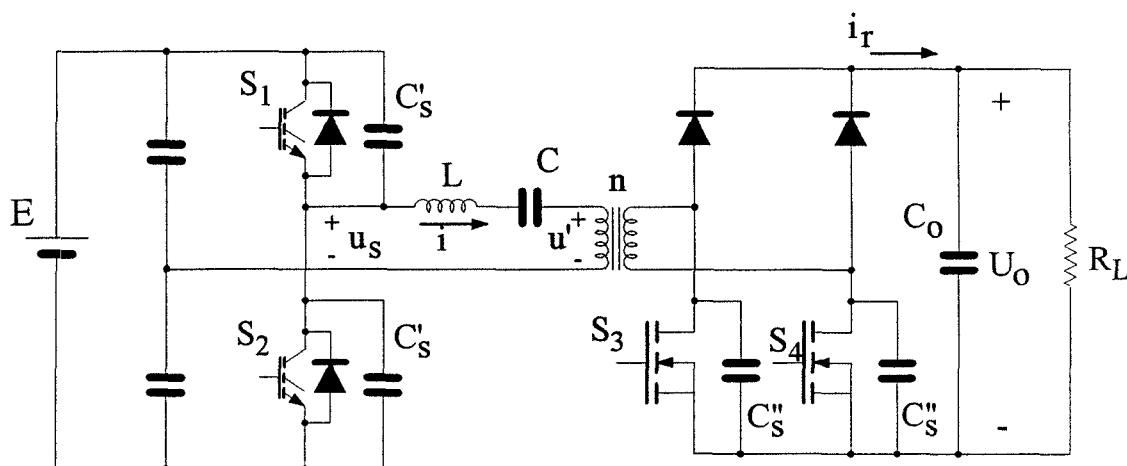


Fig.1 - Converter topology

the output voltage can be increased above the intrinsic limit (step-up capability); the switching frequency can be kept constant also for the half bridge topology, or, alternatively, a limited variation of the switching frequency can be used to maintain the energy stored in the resonant link at constant level. This allows very fast response to load step variations and ensures zero-voltage commutations even at no-load.

The proposed topology, which is presented in the half-bridge configuration, is well suited for line-rectified applications allowing use of standard 600V components and switch drivers. Moreover, the step-up operating mode can be profitably exploited in single phase insulated PFC applications, where rectified voltage assumes lower values than the output one.

An experimental prototype, rated for 600W output power, is currently under test.

## II. CIRCUIT CONFIGURATION AND BASIC OPERATION

Fig.1 shows the circuit configuration of the proposed topology of series resonant converter. The circuit includes dc power supply ( $E$ ), half-bridge primary-side converter (inverter), resonant path ( $L$ ,  $C$ ), isolation transformer, secondary-side converter (rectifier), output capacitive filter ( $C_D$ ) and load resistor ( $R_L$ ). Snubber capacitors ( $C_S$ ) are represented too.

As switch current reversal is required, all converter switches must have freewheeling diodes. In the scheme of Fig.1, IGBT switches have external freewheeling diodes, while Mosfet switches utilize intrinsic body diode.

The converter is operated above the resonant frequency, which means that switches are turned-off while carrying current. Zero voltage turn-off commutations are ensured by means of capacitive snubbers which are charged by the resonant link current. Moreover, every switch is turned on when the corresponding freewheeling diode is conducting, ensuring zero voltage and zero current turn-on. However, lossless commutations are achieved only providing that the resonant current, during commutation, is high enough to completely discharge the snubber capacitors  $C_S$ .

The primary-side converter has the usual half-bridge topology. In particular, the two switches are operated at square wave with suitable dead time between the two driving commands. The corresponding inverter output voltage  $u_s$ , which is applied to the resonant circuit, is shown in Fig.2 together with the converter main waveforms. Due to operation slightly above resonant frequency, the resulting resonant current  $i$  is lagging the inverter output voltage and is almost sinusoidal. Its amplitude can be controlled by varying the switching frequency; the higher the switching frequency, the lower the resonant current and the converter output power are.

The secondary-side converter is the rectifier stage. Here, two additional switches are connected in place of the lower side diodes of the usual full-wave rectifier, allowing control of the current delivered to the load. While these two switches are kept off, the Mosfet body diodes ensure the rectifying action, and maximum power transfer takes place. In this situation, the converter behaves as a standard series resonant converter. Instead, when the two switches are turned on, the transformer secondary winding is short circuited, and the rectified current, injected in the output filter, becomes zero. By properly modulating these switches, rectified current can be controlled, allowing converter operation down to no-load when the two rectifier switches are kept always closed. In this case, the resonant link current tends to increase but it can be controlled by increasing the inverter switching frequency thus regulating the energy stored in the resonant path.

The operation of the rectifier switches can be better understood by looking at the waveforms shown in Fig.2. The two switches of the rectifier stage are operated alternatively: during the positive half-cycle of the resonant current the body diode of  $S_4$  is conducting, thus  $S_4$  can be turned on at zero voltage and zero current. The switch is then kept closed for an additional time  $\delta T_r$  after current reversal, thus causing a short circuit of the transformer secondary winding with consequent zeroing of voltage  $u'$ . During the resonant current negative half-cycle, rectifier operation remains the same except that now switch  $S_3$  is involved. The rectifier controller regulates the interval  $\delta T_r$  so as to maintain the output voltage at a given level. This way the inverter and the rectifier controllers do not require synchronization signals (which call for isolation) between them, as the secondary side controller can take the synchronization directly on the secondary side voltage. Thus, two independent controllers can be used.

Conventional series resonant converters have an intrinsic limitation on the output voltage, i.e. the average of the rectified voltage on the transformer primary side cannot exceed the dc link voltage ( $E/2$  in the half-bridge topology). In the proposed converter, instead, due to the rectifier switches modulation, this limit can be overcome by increasing the duty cycle, and greater output voltages can be achieved (as explained in the next paragraph). This feature can be usefully utilized in single phase PFCs, where the input (rectified) voltage varies from zero to the maximum of the line voltage.

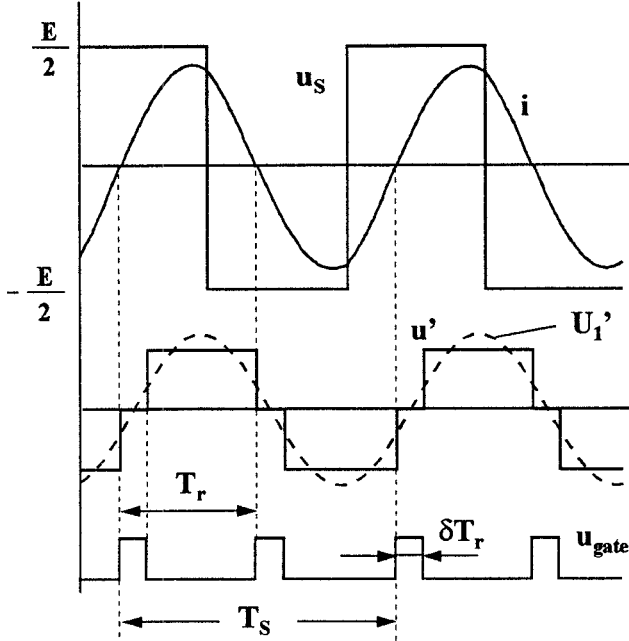


Fig.2 - Converter main waveforms. From top to bottom: inverter output voltage  $u_s$ , resonant current  $i$ , rectifier voltage  $u'$  with its fundamental component  $U_1'$  and rectifier switches duty-cycle  $\delta T_r$

### III. CONVERTER BASIC EQUATIONS

The converter basic operation can be easily described in the hypothesis of a switching frequency close to the resonant frequency and negligible converter losses. Moreover, without loss of generality, we assume a unity transformer turns ratio. With these assumptions, the resulting resonant link current is practically sinusoidal, and the power transferred to the load is related to the fundamental component of the rectifier stage input voltage  $U_1'$ , shown dashed in Fig.3 together with other converter waveforms. This voltage component results to be lagging respect to the resonant current by an angle  $\alpha$ , shown also in Fig.3, which is simply related to the rectifier switches duty-cycle  $\delta$  by the following formula:

$$\alpha = \delta \cdot \frac{\pi}{2} \quad (1)$$

Voltage  $U_1'$  can be determined from the three-level waveform of the rectifier input voltage  $u'$ , and its amplitude  $\hat{U}$  is given by:

$$\hat{U} = \frac{4}{\pi} U_0 \cdot \cos\left(\frac{\delta \cdot \pi}{2}\right) \quad (2)$$

The load dc current  $I_0$ , must equals the average component of the rectified current  $i_r$  shown also in Fig.3, i.e.

$$I_0 = \frac{\hat{I}}{\pi} \cdot (1 + \cos(\delta \cdot \pi)) \quad (3)$$

where  $\hat{I}$  is the rectifier current peak value.

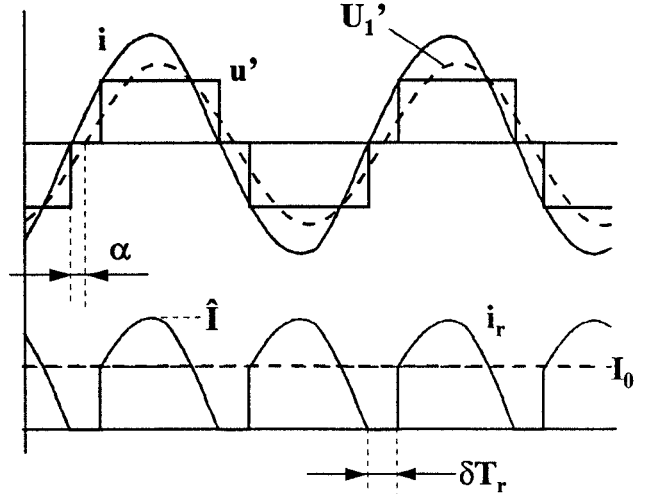


Fig.3 - Converter main waveforms. From top to bottom: resonant current  $i$ , rectifier voltage  $u'$  with its fundamental component  $U_1'$  and rectifier current  $i_r$

Neglecting the harmonics of the resonant current, only the fundamental one will be considered. In this way, the rectifier stage can be substituted by an equivalent ac load made by a resistance, which takes into account the overall power transferred to the dc load, in parallel with a capacitor which accounts for the displacement  $\alpha$  between rectifier input voltage fundamental component and current.

From (2) and (3), the equivalent resistance is given by the ratio of rectifier input ac voltage  $\hat{U}$  and the in-phase term of the ac current  $\hat{I}$ :

$$R_{eq} = \frac{\hat{U}}{\hat{I} \cdot \cos\left(\frac{\delta \cdot \pi}{2}\right)} = \frac{8}{\pi^2} \cdot \cos^2\left(\frac{\delta \cdot \pi}{2}\right) \cdot R_L \quad (4)$$

Similarly, the equivalent capacitor has an impedance which is given by:

$$X_{Ceq} = \frac{\hat{U}}{\hat{I} \cdot \sin\left(\frac{\delta \cdot \pi}{2}\right)} = \frac{R_{eq}}{\tan\left(\frac{\delta \cdot \pi}{2}\right)} \quad (5)$$

Let us assume, for a simplified analysis, a small values for  $\delta$ , ( $\delta < 0.3$ ). In this case, the equivalent capacitor impedance results much higher than the resistance  $R_{eq}$  and can be neglected. Thus, the quality factor of the resonant circuit can be expressed in terms of  $R_{eq}$  and results:

$$Q = \frac{Z_0}{R_{eq}} = \frac{Q_0}{\cos^2\left(\frac{\delta \cdot \pi}{2}\right)} \quad (6)$$

Where  $Q_0$  is the quality factor obtained when  $\delta = 0$ :

$$Q_0 = \frac{\sqrt{L/C}}{\frac{8}{\pi^2} \cdot R_L} \quad (7)$$

which equals the usual expression of the quality factor of a series resonant converter.

At the resonant frequency, the resonant link impedance zeroes and the fundamental component of inverter output voltage, which is given by:

$$\hat{U}_S = \frac{4 E}{\pi 2} \quad (8)$$

equals that at the input of the rectifier stage (2) which reaches its maximum value. From (2) and (8), the value of the output dc voltage results:

$$U_0(\delta) = \frac{E/2}{\cos\left(\frac{\delta \cdot \pi}{2}\right)} \quad (9)$$

The above equation shows the step-up effect which can be obtained by varying the duty-cycle  $\delta$  of the rectifier switches. So, the intrinsic output voltage limitation of the classic series resonant converter can be overcome for a proper design of the converter. This interesting feature is actually investigated in the converter application as insulated PFC.

For greater values of  $\delta$ , the above equation becomes less accurate and converter behaviour and design can be profitably exploited by analyzing the converter performance in the state plane. Resonant circuit equations can be written as:

$$\begin{aligned} \frac{d u_C}{d t} &= \frac{i}{C} \\ \frac{d u_{C_{eq}}}{d t} &= \frac{1}{C} \left( i - \frac{u_{C_{eq}}}{R_{eq}} \right) \\ \frac{d i}{d t} &= \frac{u_S - u_C - u_{C_{eq}}}{L} \end{aligned} \quad (10)$$

which are more conveniently expressed in adimensional form by choosing proper base coefficients:

$$\begin{aligned} U_B &= E/2 && \text{base voltage} \\ I_B &= U_B / Z_0 && \text{base current} \\ \vartheta &= \omega_0 \cdot t && \text{base time} \\ Z_0 &= \sqrt{\frac{L}{C}} && \text{characteristic impedance} \\ \omega_0 &= \sqrt{\frac{1}{LC}} && \text{angular resonant frequency} \end{aligned}$$

With these assumptions, converter equations become:

$$\begin{bmatrix} \frac{\partial u_{CN}}{\partial \vartheta} \\ \frac{\partial u_{C_{eqN}}}{\partial \vartheta} \\ \frac{\partial i_N}{\partial \vartheta} \end{bmatrix} = \begin{bmatrix} 0 & 0 & 1 \\ 0 & Q \frac{C}{C_{eq}} & \frac{C}{C_{eq}} \\ -1 & -1 & 0 \end{bmatrix} \begin{bmatrix} u_{CN} \\ u_{C_{eqN}} \\ i_N \end{bmatrix} + \begin{bmatrix} 0 \\ 0 \\ u_{SN} \end{bmatrix} \quad (11)$$

where subscript N means normalized terms.

Capacitance ratio in (11) can be rewritten in terms of independent variables in the form:

$$\frac{C}{C_{eq}} = \frac{\omega}{\omega_0} \frac{1}{Q_0} \frac{\cos^3\left(\frac{\delta\pi}{2}\right)}{\sin\left(\frac{\delta\pi}{2}\right)} \quad (12)$$

where  $\omega$  is the angular switching frequency.

From (11) it is possible to obtain the normalized output dc voltage versus normalized angular switching frequency for different values of duty cycle  $\delta$  and constant load resistor  $R_L$  as reported in Fig.4. It is possible to note the increase of the quality factor when  $\delta$  increases and the small change in the resonant frequency due to the effect of the equivalent capacitor  $C_{eq}$  neglected in the simplified analysis. As an example, with  $\delta = 0.7$ , the value of quality factor  $Q$  increases about five times, while the resonance frequency moves no more than 5%.

Fig.5 reports the normalized output dc voltage versus rectifier switches duty cycle  $\delta$  at a given switching frequency. The curves drawn for high normalized frequency show an initial increasing behaviour with  $\delta$  and, for higher value of  $\delta$ , the slope reverses. This fact, which is more evident at higher switching frequency than at lower one, is due to the quick increment of the quality factor with  $\delta$  which reduces the converter gain at high frequency.

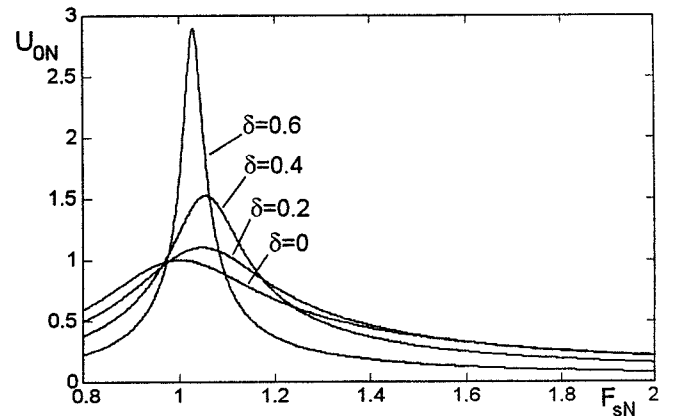


Fig.4 - Normalized output voltage  $U_{ON}$  as a function of normalized switching frequency  $F_{sN}$ , for different values of rectifier switches duty-cycle  $\delta$

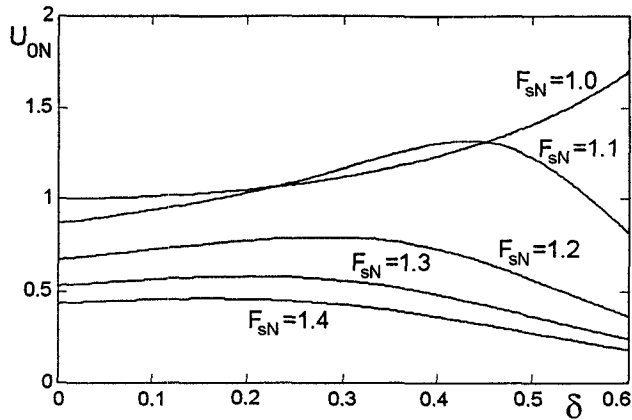


Fig.5 - Normalized output voltage  $U_{ON}$  as a function of rectifier switches duty-cycle  $\delta$ , for different values of normalized switching frequency  $F_{sN}$

#### IV. SIMULATED AND EXPERIMENTAL RESULTS

Converter behaviour was firstly investigated by simulation in order to well understand its features. After this an experimental prototype was built with the aim to test its performances. The converter has been designed according to the following specifications:

- DC output voltage = 48V
- DC output current = 12A
- DC input voltage = 300V
- Resonant frequency = 47.4kHz

Moreover the following parameters has been chosen:

- Resonant inductor = 240 $\mu$ H
- Resonant capacitor = 47nF
- Inverter snubber capacitors = 2.7nF
- Rectifier snubber capacitors = 4.7nF

In the inverter stage two IGBTs have been selected, while for the rectifier MOSFET switches are adopted which allow rectifier losses reduction if kept closed when MOSFET body diode conduct reverse current.

Fig.6 shows inverter main waveforms at steady state. The inverter is operated at 56kHz square wave. Resonant link current is quite sinusoidal as the converter operates small above the resonant frequency. Rectifier input voltage is kept to zero, after the current reversing, giving a duty-cycle  $\delta$  regulated to 18%. More detailed switching behaviour are shown in Fig.7, where previous waveforms are expanded and the effect of rectifier and inverter snubbers is more evident.

Fig.8 shows inverter main waveforms at steady state when operated in step-up mode. The duty-cycle  $\delta$  is regulated ad 36% and the output rectified voltage becomes 15% greater than the inverter supply voltage.

Fig.9 shows the rectifier input voltage and the resonant current together with the rectifier switches

commands. These signals differ from that of Fig.2 because both switches are closed also when corresponding diode is conducting, in order to reduce conduction losses, and then kept in the on state with positive current for about 3 $\mu$ s, ( $\delta = 36\%$ ).

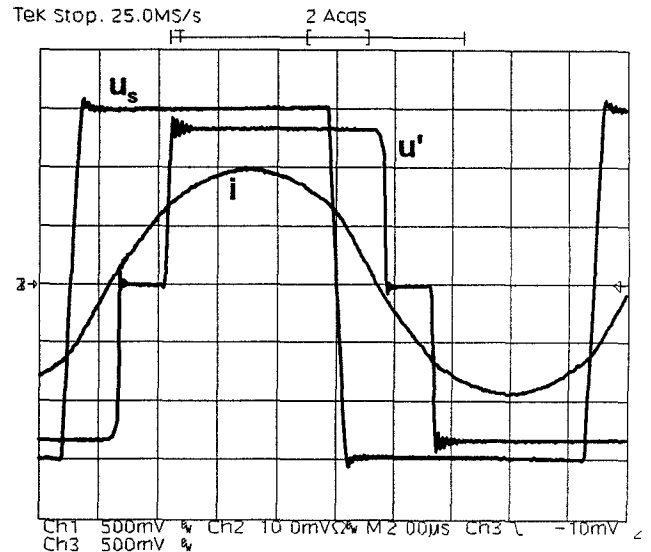


Fig.6 - Converter main waveforms in step-down operating mode: inverter output voltage  $u_s$  [50V/div], rectifier input voltage  $u'$  [50V/div], resonant link current  $i$  [2.5A/div],  $F_s = 56$ kHz,  $\delta = 18\%$ .

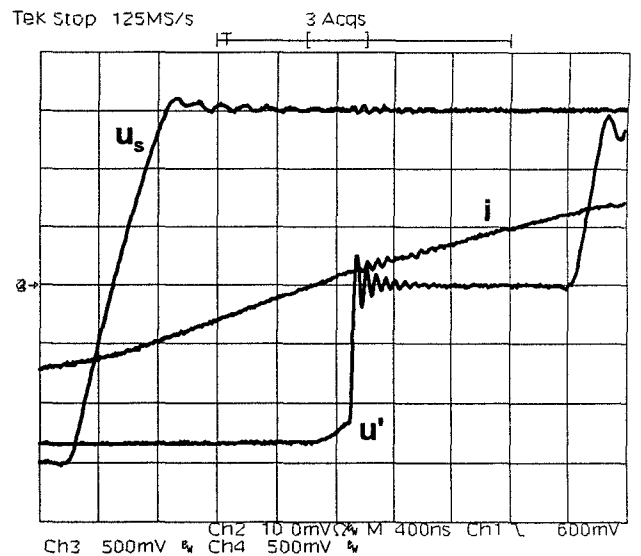


Fig.7 - Switching behaviour of converter waveforms: inverter output voltage  $u_s$  [50V/div], rectifier input voltage  $u'$  [50V/div], resonant link current  $i$  [2.5A/div],  $F_s = 56$ kHz,  $\delta = 18\%$ .

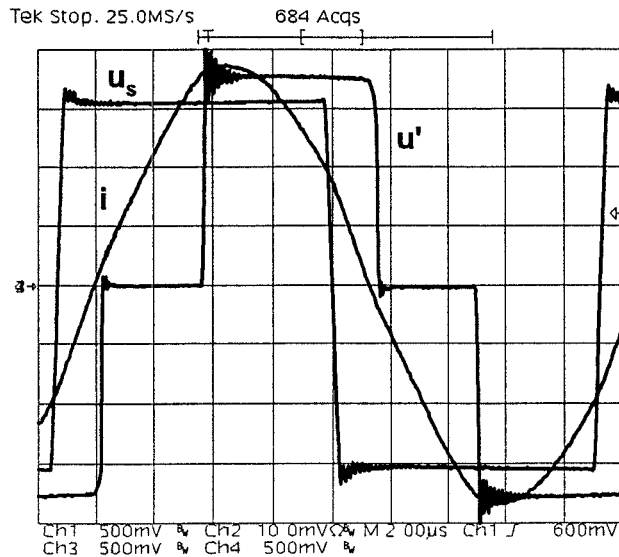


Fig.8 - Converter main waveforms in the step-up operating mode: inverter output voltage  $u_s$  [50V/div], rectifier input voltage  $u'$  [50V/div], resonant link current  $i$  [2.5A/div],  $F_s = 53.6\text{kHz}$ ,  $\delta = 36\%$ .

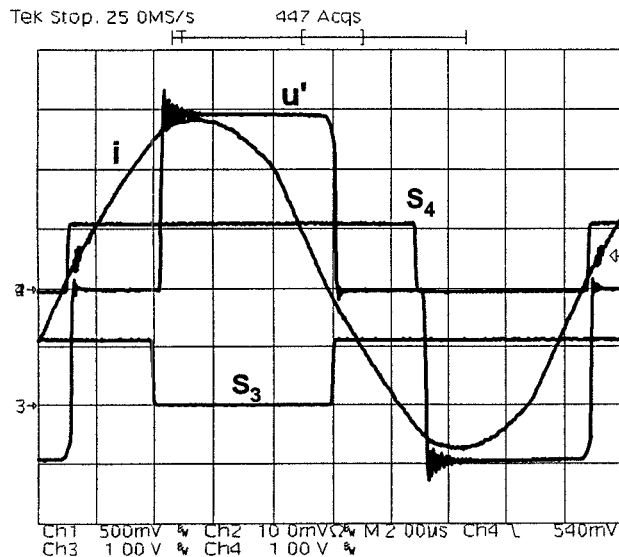


Fig.9 - Converter main waveforms: rectifier input voltage  $u'$  [50V/div], resonant link current  $i$  [2.5A/div], rectifier switch commands  $S_3$  and  $S_4$  [10V/div],  $F_s = 56\text{kHz}$ ,  $\delta = 34\%$ .

## V. CONCLUSIONS

A series resonant converters topology is presented which employs two additional switches in the rectifier stage. This modification of the classic converter topology

allows output voltage control down to no load condition and boost operation while maintaining soft switching in any operating condition.

Several kinds of control are allowed depending on optimization goal.

An experimental prototype of a half-bridge converter rated for 48V, 600W output power has been tested demonstrating the theoretical converter capability.

## References

1. R.Oruganti, F.C.Lee: "Resonant power processor: Part I - State plain analysis". IEEE-IAS '84 Annual Meeting, pp. 860-867
2. R.Oruganti, F.C.Lee: "Resonant power processor: Part II - Methods of control". IEEE-IAS '84 Annual Meeting, pp. 868-878
3. V.Sendanyoye, K.Al-Haddad, V.Rajagopalan: "Optimal trajectory control strategy for improved dynamic response of series resonant converter". IEEE-IAS '90 Annual Meeting. Seattle, October 1990, pp. 1236-1242.
4. M.G.Kim, D.S.Lee, M.J.Youn: "A new state feedback control of resonant converters". IEEE Transaction on Industrial Electronics, Vol.38, N.3, June 1991, pp.173-179.
5. S.Sivakumar, K.Natarajan, A.M.Sharaf: "Optimal trajectory control of series resonant converter using modified capacitor voltage control technique". IEEE-PESC '91 Annual Meeting, Cambridge-Boston, June 1991, pp.752-759.
6. M.G.Kim, M.J.Youn: "A discrete time domain modeling and analysis of controlled series resonant converter". IEEE Transaction on Industrial Electronics, Vol.38, N.1, February 1991, pp.32-40.
7. L.Rossetto: "A simple control technique for series resonant converters". IEEE Transaction on Power Electronics, Vol.11, n.4, July, 1996, pp.554-560.
8. G.B.Joung, C.T.Rim, G.H.Cho: "Modeling of quantum series resonant converters controlled by integral cycle mode". IEEE-IAS '88 Annual Meeting, Pittsburgh, October 1988, pp. 821-826.